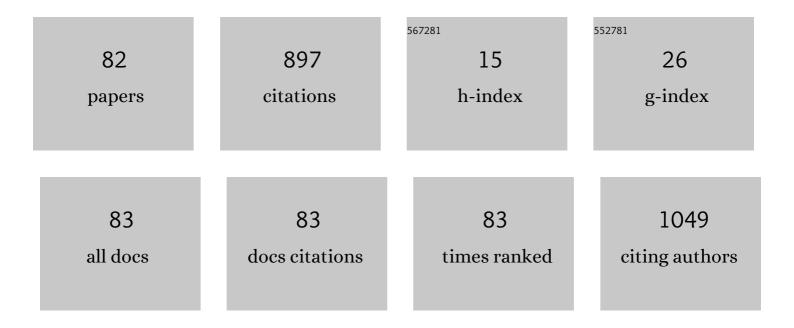
List of Publications by Year in descending order

Source: https://exaly.com/author-pdf/7476780/publications.pdf Version: 2024-02-01



#	Article	IF	CITATIONS
1	History and future of human cadaver preservation for surgical training: from formalin to saturated salt solution method. Anatomical Science International, 2016, 91, 1-7.	1.0	116
2	REVIEW ARTICLE: Patterns of Infiltration of Lymphocytes into the Testis Under Normal and Pathological Conditions in Mice. American Journal of Reproductive Immunology, 2008, 59, 55-61.	1.2	61
3	Experimental autoimmune orchitis as a model of immunological male infertility. Medical Molecular Morphology, 2012, 45, 185-189.	1.0	50
4	Site specificity of mechanical and structural properties of human fascia lata and their gender differences: A cadaveric study. Journal of Biomechanics, 2018, 77, 69-75.	2.1	38
5	Acetamiprid Accumulates in Different Amounts in Murine Brain Regions. International Journal of Environmental Research and Public Health, 2016, 13, 937.	2.6	32
6	Low-dose exposure to di-(2-ethylhexyl) phthalate (DEHP) increases susceptibility to testicular autoimmunity in mice. Reproductive Biology, 2015, 15, 163-171.	1.9	30
7	Site- and sex-differences in morphological and mechanical properties of the plantar fascia: A supersonic shear imaging study. Journal of Biomechanics, 2019, 85, 198-203.	2.1	29
8	Developing spray-freeze-dried particles containing a hyaluronic acid-coated liposome–protamine–DNA complex for pulmonary inhalation. International Journal of Pharmaceutics, 2020, 583, 119338.	5.2	29
9	Contribution of IL-12/IL-35 Common Subunit p35 to Maintaining the Testicular Immune Privilege. PLoS ONE, 2014, 9, e96120.	2.5	24
10	Effect of a Magnetic Field on Drosophila under Supercooled Conditions. PLoS ONE, 2012, 7, e51902.	2.5	22
11	Early Postnatal Exposure to a Low Dose of Decabromodiphenyl Ether Affects Expression of Androgen and Thyroid Hormone Receptor-Alpha and Its Splicing Variants in Mouse Sertoli Cells. PLoS ONE, 2014, 9, e114487.	2.5	21
12	Postinflammation stage of autoimmune orchitis induced by immunization with syngeneic testicular germ cells alone in mice. Medical Molecular Morphology, 2012, 45, 35-44.	1.0	20
13	Histopathology of the tubuli recti at the start of experimental autoimmune orchitis in mice. Medical Molecular Morphology, 2009, 42, 230-235.	1.0	19
14	Neonatal estrogen treatment with β-estradiol 17-cypionate induces in post-pubertal mice inflammation in the ductuli efferentes, epididymis, and vas deferens, but not in the testis, provoking obstructive azoospermia. Medical Molecular Morphology, 2014, 47, 21-30.	1.0	17
15	Morphological and mechanical properties of the human triceps surae aponeuroses taken from elderly cadavers: Implications for muscle-tendon interactions. PLoS ONE, 2019, 14, e0211485.	2.5	17
16	Left testicular artery arching over the ipsilateral renal vein. Asian Journal of Andrology, 2006, 8, 107-110.	1.6	15
17	Gosha-Jinki-Gan Recovers Spermatogenesis in Mice with Busulfan-Induced Aspermatogenesis. International Journal of Molecular Sciences, 2018, 19, 2606.	4.1	14
18	Expression of Angiopoietins and Angiogenic Signaling Pathway Molecules in Chronic Subdural Hematomas. Journal of Neurotrauma, 2020, 37, 2493-2498.	3.4	14

#	Article	IF	CITATIONS
19	Developmental ontogeny of autoantigens associated with localized autoimmunity in murine testis and epididymis. Journal of Reproductive Immunology, 2010, 87, 45-51.	1.9	13
20	Specific autoantigens identified by sera obtained from mice that are immunized with testicular germ cells alone. Scientific Reports, 2016, 6, 35599.	3.3	13
21	Lacrimal drainage anatomy in the Japanese population. Annals of Anatomy, 2019, 223, 90-99.	1.9	13
22	Acute effects of longâ€distance running on mechanical and morphological properties of the human plantar fascia. Scandinavian Journal of Medicine and Science in Sports, 2020, 30, 1360-1368.	2.9	13
23	Effect of unilateral testicular rupture on histopathology and germ cell delayed-type hypersensitivity in C3H/He and A/J mice. Journal of Reproductive Immunology, 2009, 81, 55-61.	1.9	12
24	Preservation by Desiccation of Isolated Rat Hearts for 48 Hours Using Carbon Monoxide (PCO = 4,000) Tj ETQq0	0.0.rgBT	/Oygrlock 10
25	Uncarboxylated Osteocalcin Induces Antitumor Immunity against Mouse Melanoma Cell Growth. Journal of Cancer, 2017, 8, 2478-2486.	2.5	12
26	The presence of intra-tubular lymphocytes in normal testis of the mouse. Okajimas Folia Anatomica Japonica, 2008, 85, 91-96.	1.2	11
27	Multilayered structure of the basal lamina of the tubuli recti in normal mice. Medical Molecular Morphology, 2011, 44, 34-38.	1.0	11
28	Busulfan pretreatment for transplantation of rat spermatogonia differentially affects immune and reproductive systems in male recipient mice. Anatomical Science International, 2015, 90, 264-274.	1.0	11
29	Functional evaluation of rat hearts transplanted after preservation in a high-pressure gaseous mixture of carbon monoxide and oxygen. Scientific Reports, 2016, 6, 32120.	3.3	11
30	Site dependent elastic property of human iliotibial band and the effect of hip and knee joint angle configuration. Journal of Biomechanics, 2020, 109, 109919.	2.1	11
31	Pathological effect of arterial ischaemia and venous congestion on rat testes. Scientific Reports, 2017, 7, 5422.	3.3	10
32	Cardioprotection via Metabolism for Rat Heart Preservation Using the High-Pressure Gaseous Mixture of Carbon Monoxide and Oxygen. International Journal of Molecular Sciences, 2020, 21, 8858.	4.1	10
33	Physical disuse contributes to widespread chronic mechanical hyperalgesia, tactile allodynia, and cold allodynia through neurogenic inflammation and spino-parabrachio-amygdaloid pathway activation. Pain, 2020, 161, 1808-1823.	4.2	10
34	Serum Autoantibodies in Mice Immunized with Syngeneic Testicular Germ Cells Alone. American Journal of Reproductive Immunology, 2013, 70, 509-517.	1.2	9
35	Framework for visual-feedback training based on a modified self-organizing map to imitate complex motion. Proceedings of the Institution of Mechanical Engineers, Part P: Journal of Sports Engineering and Technology, 2020, 234, 49-58.	0.7	9
36	Track distance runners exhibit bilateral differences in the plantar fascia stiffness. Scientific Reports, 2021, 11, 9260.	3.3	9

#	Article	IF	CITATIONS
37	Anatomical Relationship between Bl23 and the Posterior Ramus of the L2 Spinal Nerve. Acupuncture in Medicine, 2016, 34, 95-100.	1.0	8
38	Location of the myoneural junction of the inferior oblique muscle: An anatomic study. Annals of Anatomy, 2020, 227, 151429.	1.9	8
39	Visual recognition of mirror, video-recorded, and still images in rats. PLoS ONE, 2018, 13, e0194215.	2.5	8
40	Multiple renal vessels associated with testicular vessels. Surgical and Radiologic Anatomy, 2011, 33, 637-639.	1.2	6
41	Induction of experimental autoimmune orchitis by immunization with xenogenic testicular germ cells in mice. Journal of Reproductive Immunology, 2017, 121, 11-16.	1.9	6
42	Anorectal autotransplantation in a canine model: the first successful report in the short term with the non-laparotomy approach. Scientific Reports, 2014, 4, 6312.	3.3	5
43	Morphological study of the neurovascular bundle to elucidate nerve damage in pelvic surgery. International Journal of Colorectal Disease, 2016, 31, 503-509.	2.2	5
44	A case of an additional right external iliac vein surrounding the right external iliac artery and lacking the right common iliac vein. Anatomical Science International, 2016, 91, 106-109.	1.0	5
45	Therapeutic effects of diclofenac, pregabalin, and duloxetine on disuse-induced chronic musculoskeletal pain in rats. Scientific Reports, 2018, 8, 3311.	3.3	5
46	Interlower and postlower eyelid retractor fat pads: a cadaveric microscopic study. British Journal of Ophthalmology, 2018, 102, 404-406.	3.9	5
47	Preservation of rat limbs by hyperbaric carbon monoxide and oxygen. Scientific Reports, 2018, 8, 6627.	3.3	5
48	High-Pressure Carbon Monoxide and Oxygen Mixture is Effective for Lung Preservation. International Journal of Molecular Sciences, 2019, 20, 2719.	4.1	5
49	Spraying urea solution reduces formaldehyde levels during gross anatomy courses. Anatomical Science International, 2019, 94, 209-215.	1.0	5
50	Development of heterotopic transplantation of the testis with the epididymis to evaluate an aspect of testicular immunology in rats. PLoS ONE, 2017, 12, e0177067.	2.5	4
51	Evaluation of the pressure on the dorsal surface of the distal radius using a cadaveric and computational model: clinical considerations in intersection syndrome and Colles' fracture. Anatomical Science International, 2020, 95, 38-46.	1.0	4
52	The Role of Overriding Preseptal Orbicularis Oculi Muscle in Development of Involutional Lower Eyelid Entropion. Journal of Craniofacial Surgery, 2020, 31, 573-576.	0.7	4
53	Anatomical relationship between the sagittal band and extensor tendon of the thumb: a focus on variations of the extensor pollicis brevis tendon insertion. Anatomical Science International, 2020, 95, 356-362.	1.0	4
54	Glucose infusion suppresses acute restraint stress-induced peripheral and central sympathetic responses in rats. Autonomic Neuroscience: Basic and Clinical, 2022, 239, 102957.	2.8	4

#	Article	IF	CITATIONS
55	A left testicular artery arising from a middle mesenteric artery. Clinical Anatomy, 2011, 24, 266-267.	2.7	3
56	A case of pancake kidney with a single ureter in the retroperitoneal space. Anatomical Science International, 2018, 93, 563-565.	1.0	3
57	Different effects of partial pressure in a high-pressure gaseous mixture of carbon monoxide and oxygen for rat heart preservation. Scientific Reports, 2019, 9, 7480.	3.3	3
58	Relationship of segmental variations in the human lumbar plexus to the length of the 12th rib. Annals of Anatomy, 2021, 233, 151592.	1.9	3
59	Investigation of the association between human fascia lata thickness and its neighboring tissues' morphology and function using Bâ€mode ultrasonography. Journal of Anatomy, 2021, 239, 1114-1122.	1.5	3
60	Efficacy of urea solution reperfusion to a formalin-embalmed cadaver for surgical skills training. Anatomical Science International, 2022, 97, 264-272.	1.0	3
61	A case of a cystic artery arising from the superior mesenteric artery with abnormal branching of the celiac trunk. BMC Research Notes, 2017, 10, 526.	1.4	2
62	Positional relationship between medial canthal tendon and common canalicular orifice: A cadaveric study. Annals of Anatomy, 2020, 227, 151432.	1.9	2
63	Heat shock protein A4L is a potent autoantigen for testicular autoimmunity in mice. Journal of Reproductive Immunology, 2021, 145, 103318.	1.9	2
64	Efficacy of Methotrexate on Rat Knee Osteoarthritis Induced by Monosodium Iodoacetate. Journal of Inflammation Research, 2021, Volume 14, 3247-3259.	3.5	2
65	Thyroid Gland Flap for Minimally Invasive Reconstructive Head and Neck Surgery. Plastic and Reconstructive Surgery - Global Open, 2020, 8, e3297.	0.6	2
66	A rare third head of the biceps femoris in the posterior thigh. Anatomical Science International, 2021, 96, 157-160.	1.0	1
67	Anorectal Transplantation. Annals of Surgery, 2021, Publish Ahead of Print, .	4.2	1
68	Cytoprotective Autophagy Induction by Imatinib Mesylate In Non-BCR-ABL Expressing Cells. Blood, 2010, 116, 4937-4937.	1.4	1
69	Anatomical Study on the Left Brachiocephalic Vein Compression by Using CT Image. The Japanese Journal of Phlebology, 2018, 29, 323-327.	0.0	1
70	Fruit Fly, Drosophila melanogaster, as an In Vivo Tool to Study the Biological Effects of Proton Irradiation. Radiation Research, 2020, 194, 143.	1.5	1
71	The left brachiocephalic vein â€~spur': A cadaveric and contrast computed tomography study. Phlebology, 2019, 34, 690-697.	1.2	0
72	The superoxide scavenger tempol attenuates DNA oxidative injury and spontaneous pain-like behavior in chronic post-cast pain model rats. Biochemical and Biophysical Research Communications, 2020, 533, 745-750.	2.1	0

#	Article	IF	CITATIONS
73	Analysis of the positional relationship between the left brachiocephalic vein and its surrounding vessels via computed tomography scan: A retrospective study. Phlebology, 2020, 35, 416-423.	1.2	0
74	Fruit Fly, Drosophila melanogaster, as an In Vivo Tool to Study the Biological Effects of Proton Irradiation. Radiation Research, 2020, , .	1.5	0
75	Evaluation of a Framework for Visual-Feedback Training Based on a Modified Self-Organizing Map Using Sensing Information Including Muscle Activity. Proceedings (mdpi), 2020, 49, .	0.2	0
76	Autophagy and Apoptosis Are Induced Simultaneously in Leukemia Cells by Vitamin K2 Blood, 2006, 108, 4373-4373.	1.4	0
77	Combined Treatment with Bortezomib Plus Bafilomycin A1 Enhances Cytocidal Effect along with Induction of ER Stress In Myeloma Cells: Crosstalk Among Proteasome, Autophagy-Lysosome, and ER Stress. Blood, 2010, 116, 4058-4058.	1.4	0
78	1B41 Oxygenation of rewarming machine perfusion for resuscitate liver function. The Proceedings of the Bioengineering Conference Annual Meeting of BED/JSME, 2015, 2015.27, 85-86.	0.0	0
79	Development of a feedback training system with visualization of motion information using self-organizing map. The Proceedings of the Symposium on Sports and Human Dynamics, 2018, 2018, D-9.	0.0	0
80	Wrist immobilization position contributing to stabilize a bone fracture fragment after a distal radius fracture. The Proceedings of Mechanical Engineering Congress Japan, 2018, 2018, J0240402.	0.0	0
81	Development of anatomical dynamic model of shoulder joint and surrounding tissue. The Proceedings of the Symposium on Sports and Human Dynamics, 2019, 2019, C-32.	0.0	0
82	Muscle Spindles in the Levator Palpebrae Superioris Muscle of Human Adults. Journal of Craniofacial Surgery, 2021, 32, 1532-1534.	0.7	0